Published by Institute of Physics Publishing

Journal of Physics: Condensed Matter

Top Papers 2003 Showcase highlights the leading and most frequently downloaded papers, letters and topical reviews to Journal of Physics: Condensed Matter, arguably the world's most authoritative source of topical information for condensed matter physicists and materials and surface scientists. Journal of Physics: Condensed Matter covers experimental and theoretical studies of the structural, thermal, mechanical, electrical, magnetic and optical properties of condensed matter and is published 50 times per year by Institute of Physics Publishing.

We welcome papers and submissions from authors who have research interests in these areas. Authors can benefit from rapid receipt-to-publication times, a rising impact factor and a large and growing world wide readership both in print and on-line. On average papers are downloaded on-line over 100 times via our award winning Electronic Journals service.

For more information on the submission process and to view the latest published papers from Journal of Physics: Condensed Matter visit **www.iop.org/EJ/journal/JPhysCM**

PAPERS

REVIEWS

Inside you will find synopses of all the top papers and reviews listed above, together with details of where to find the full articles Ł Ł Ł Ł

Magnetic nanostructures

Static and dynamic magnetic behaviour of iron nanoclusters on magnetic substrates

C Binns, F Sirotti, H Cruguel, S H Baker, P Prieto, J D Bellier and S C Thornton

J. Phys.: Condens. Matter
15 No 25 (2 July 2003) 4287–4299

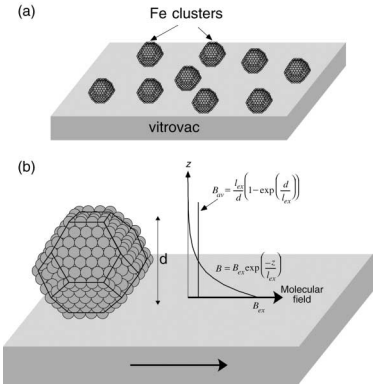

Schematic diagram of the molecular field within Fe clusters adsorbed on vitrovac due to the exchange interaction at the contact point between the clusters and the substrate.

In magnetic nanoparticles containing a few to a few thousand atoms, the exchange length is significant compared to the cluster diameter. This produces a number of interesting and technically useful effects, e.g. in magnetic recording applications. Even when deposited on a surface or embedded in a matrix, 3d transition metal clusters have a significantly higher magnetic moment per atom relative to the bulk. C Binns' group at Leicester with co-workers at LURE Orsay, Sincrotrone Trieste and Madrid report static and dynamic measurements of Fe nanoclusters of 140–270 atoms, deposited in situ onto amorphous vitrovac substrates, using a gas aggregation source. Magnetic behaviour was determined specifically within the Fe clusters, independent of the substrate or coating materials.

Magnetic linear dichroism in the angular distribution (MLDAD) of the Fe 3p core level photoemission gave the static magnetization of the cluster films in the exchange field of the substrates as a function of coverage. The switching dynamics were studied on the nanosecond timescale by time-resolved spin-polarized photoemission. The MLDAD signal at saturation of dense cluster films with several cluster layers was ~5% higher than an MBE-grown film, indicating an enhanced spin moment even when clusters are in contact. Coating an exposed sub-monolayer cluster layer with Co increases the Fe MLDAD signal by 35%, indicating a substantially increased magnetic moment within the Fe clusters. At low coverages, below the percolation threshold, the sample showed the same switching dynamics as in the clean substrate. Near the percolation threshold, however, a significant acceleration of the magnetic reversal was seen, with a fast component due to a reversal propagating through the cluster film. On average, each cluster switches in about 10 ns.

Microstructure of gels

Microstructure of dense colloid–polymer suspensions and gels

S A Shah, Y-L Chen, S Ramakrishnan, K S Schweizer and C F Zukoski

J. Phys.: Condens. Matter
15 No 27 (16 July 2003) 4751–4778

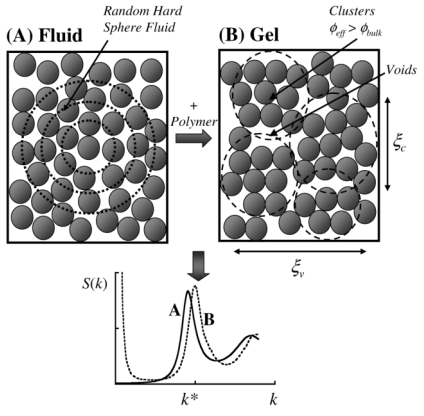

An illustration of (A) a hard-sphere solution and (B) interpenetrating, polydisperse, dense percolated clusters of an average size ξ_c. The surrounding voids or heterogeneities have a characteristic length of $\xi_v \sim 5$–$8D$ where D is the colloid diameter. Also shown is a schematic illustrating changes in the structural correlations as equilibrium fluids transform to dense gels.

Suspensions which undergo a fluid-to-gel transition are of enormous technological significance, partly because the gel microstructure and mechanical properties can be controlled. Recent studies show that gels can form from the homogeneous fluid phase with increasing strength of interparticle attraction when the range of the attraction is less than about a tenth of a particle radius, *R*. The suspension flow properties change from liquid-like to solid-like, since relaxation times grow to be longer than times of experimental observation. The material displays a dynamic yield stress.

A gel is a non-ergodic, space-filling soft solid where long-range diffusive motion is arrested. A model system for systematically changing the strength and range of the interparticle attractions exploits depletion attractions between hard-sphere particles by adding non-adsorbing polymers. When the polymer radius of gyration is much less than the particle radius, the range of the induced attraction is small. At polymer concentrations well below where polymer coils begin to overlap, the suspensions gel. This non-equilibrium transition can pre-empt the equilibrium fluid–fluid and fluid–crystal phase transitions, or occur in a two-phase coexistence region. Gelation bears some similarities to the hard-sphere glass transition which occurs at a particle volume fraction of about 0.58.

C Zukowski's group at Urbana describes measurements of the collective structure factor of dense colloidal suspensions in the fluid and gel states produced by adding small non-adsorbing polymer such that the radius of gyration lies between 5% and 8% of *R*. Pinhole-collimated ultra-small-angle x-ray scattering (USAXS) is employed. As the polymer concentration is increased at fixed volume fraction, excellent quantitative agreement is demonstrated in the fluid phase with the parameter-free predictions of PRISM theory. Above the polymer concentration at which gels are produced, agreement is poor, showing the suspensions have fallen out of equilibrium. Upon gelation, the local cage structure is frozen, intermediate-scale fluctuations are suppressed and large small-wavevector fluctuations emerge due to heterogeneities or 'clusters'.

Oxidation of nanotubes

Photoinduced oxidation of carbon nanotubes

T Savage, S Bhattacharya, B Sadanadan, J Gaillard, T M Tritt, Y-P Sun, Y Wu, S Nayak, R Car, N Marzari, P M Ajayan and A M Rao

J. Phys.: Condens. Matter
15 No 35 (10 September 2003) 5915–5921

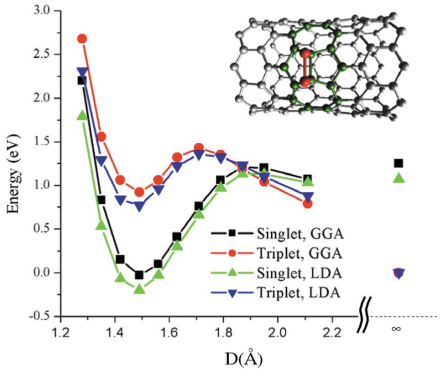

Plots of binding energy of O_2 with a (10, 0) nanotube as a function of the molecule's distance D (Å) from the nanotube surface. The binding energy of the physisorbed T state is about 0.004 eV at 3.7 Å (not shown here). The inset shows a ball and stick picture of O_2 (large atoms) bonded to a 7–5–5–7 (small atoms) defect site.

In single-walled carbon nanotube (SWNT) bundles, the sign of the thermopower proves extremely sensitive to oxygen adsorption. This has implications for practical carbon nanotube field effect transistors (CNFETs). At room temperature, thermopower values are around +45 μV K^{-1} in 'mats' of SWNT bundles doped to saturation under ambient conditions with oxygen. When oxygen is desorbed from the SWNT bundles at temperatures from 350–500 K and high vacuum (10^{-5}-10^{-8} Torr) over times from 30 minutes to 12 hours, the thermopower switches reversibly to an n-type value of about −50 μV K^{-1}. The time evolution from negative thermopower values in oxygen-desorbed SWNT mats to positive thermopower values, under ambient conditions, has a characteristic value varying from a few minutes to hours, depending on the mat thickness. Recently, p-type CNTFETs were found to convert to n-CNTFETs when annealed in vacuum. Upon re-exposure to oxygen, the p-CNTFET properties were recovered.

S Nayak's group at Rensselaer Polytechnic Institute with co-workers at Clemson, Princeton and MIT have published thermopower measurements showing that carbon nanotubes, when exposed simultaneously to UV light and oxygen, exhibit photoinduced oxidation. This they relate to a theoretical analysis for both graphene and nanotube structures with limited defect types. At least two plausible mechanisms for the experimentally observed photoinduced oxidation are proposed: (i) a lower energy barrier for the adsorption of photo-generated singlet oxygen, or (ii) the presence of defects in carbon nanotubes that may facilitate the formation of locally electron-deficient and electron-rich regions on the nanotubes, and these facilitate the adsorption of oxygen molecules on the nanotubes. Experiments with magnetic fields, like electron spin resonance (ESR), could further confirm the proposed mechanisms. Thus, the ESR of carbon nanotubes oxidized in the presence of UV light should show relatively higher concentrations of singlet oxygen compared to nanotubes oxidized under room light.

Focusing light using negative refraction

J B Pendry and S A Ramakrishna
J. Phys.: Condens. Matter
15 No 37 (24 September 2003) 6345–6364

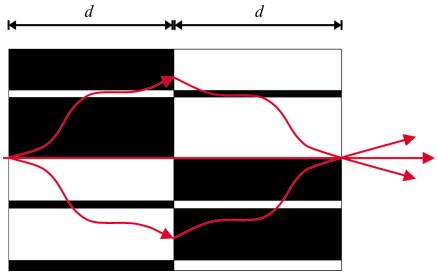

An alternative pair of complementary media, each cancelling the effect of the other. The light does not necessarily follow a straight line path in each medium, but the overall effect is as if a section of space thickness 2d were removed from the experiment.

Conventional lenses suffer from a fundamental limitation of resolution: no details finer than the wavelength of radiation can be resolved. Negative refraction lenses could do much better, and are just one example of possible novel optical devices.

Some time ago V G Veselago observed that if it were possible to realize materials with permittivity, M, and permeability, μ, both equal to -1, then a refractive index of $n = -1$ would result and a slab of the material would focus light. A negative refraction lens works according to quite different principles from a conventional lens: it builds on the idea that a negatively refracting slab, $n = -1$, is in some sense complementary to an equal thickness of vacuum and cancels its presence. This cancellation is unusually complete because the compensating effect of the slab extends not only to the radiative component of the field, but also to the evanescent near field which conveys the sub-wavelength details of the image. Ordinary lenses do not capture the near field, hence the limitations to their resolution. Lenses with this sub-wavelength focusing property are referred to as 'perfect lenses'.

The cancellation by a slab of thickness d is a special case of a much wider class of focusing: any medium can be optically cancelled by an equal thickness of material constructed to be an inverted mirror image of the medium, with M, T reversed in sign. J B Pendry and S A Ramakrishna of Imperial College, London introduce the powerful technique of coordinate transformation, mapping a known system into an equivalent system, so as to extend the result to a much wider class of structures including cylinders, spheres and intersecting planes, and hence show how to produce magnified images. All the images are 'perfect' in the sense that both the near and far fields are brought to a focus and hence reveal sub-wavelength details. The technique used in proving these results, the equivalence of coordinate transformations to a change in M and μ, is a powerful and widely applicable tool which is expected to generate even more results in the future.

Quantum transport in nanowires

Spin-dependent quantum transport effects in Cu nanowires

D M Gillingham, C Müller and J A C Bland
J. Phys.: Condens. Matter
15 No 19 (21 May 2003) L291–L296

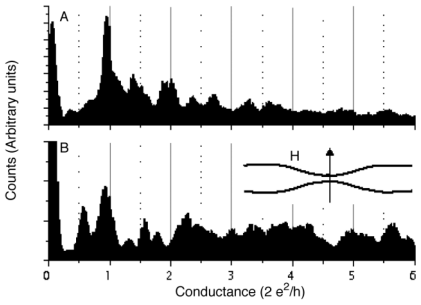

These are representative conduction histograms. They are built up from conductance versus time curves taken at room temperature in air. (A) was taken at zero applied magnetic field—it shows that the expected $2e^2/h$ quantization is dominant; however, there is a small peak at $0.5 \times 2e^2/h$ and one at $1.5 \times 2e^2/h$, showing that there is some quantization in units of e^2/h occurring. (B) was taken with a 0.5 mT magnetic field applied perpendicular to the nanowire—it shows that the e^2/h quantization has become far more dominant than in (A), the zero-field case. The inset is a schematic diagram of the field direction with respect to the nanowire.

Underlying spintronics is the proposal to use the spin of the electron instead of its electrical charge in future devices. The challenge is to achieve efficient spin injection at room temperature and to demonstrate the manipulation of electron spin in an all-electrical manner conclusively. Spintronics requires small structures to ensure that the spins act coherently, and that the electrons travel ballistically. Low-dimensional structures such as nanowires can have an electronic structure vastly different from that of the bulk material. This can be expected to be highly significant in the operation of spintronic devices.

J A C Bland's group at Cambridge has observed magnetic field-dependent quantum transport in copper nanowires. A large magnetoconductance effect arises, attributed to the formation of spin-split conduction states in the nanowire. A significant magneto-conductance effect in copper nanowires in fields of 2 mT is seen, and interpreted as being due to the spin filtering effect introduced by oxygen adsorbates modifying the electronic band structure in the nanowire. By reducing the dimensions of the active material, they find surprisingly large spin-polarized quantum conduction effects in a material which is non-magnetic in the bulk. This may offer a new approach in developing spintronic devices, differing from the current research effort devoted to developing bulk materials which have 100% spin polarization. This effect could be seen in other non-magnetic metals when formed into nanowires under the correct conditions.

Silicon-based quantum gates

Optically driven silicon-based quantum gates with potential for high-temperature operation

A M Stoneham, A J Fisher and P T Greenland
J. Phys.: Condens. Matter
15 No 27 (16 July 2003) L447–L451

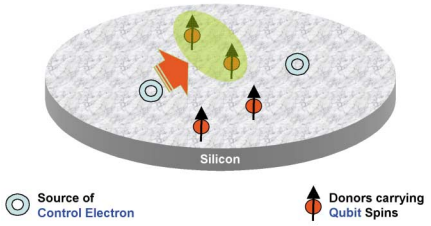

Quantum information is encoded in the electron spins of deep donors (red) in a silicon layer, the spins being manipulated optically. Entanglement is controlled using optical excitation and de-excitation of electrons from control atoms (blue rings).

In quantum information processing, challenges include quantum information storage as qubits, and quantum information manipulation. For quantum information manipulation, it suffices to have two types of universal gate: the so-called A-gates, that manipulate individual qubits, and the so-called J-gates, that control the quantum dance of one qubit with another. There would be major practical advantages if the universal quantum gates satisfied two practical criteria, namely that the processor should be silicon compatible, ideally one that might be built by largely off-the-shelf methods, and secondly that the decoherence mechanisms and key energies should be such as to allow operation at useful temperatures, ideally at room temperature, alongside conventional classical devices. Quantum behaviour is not an intrinsically low-temperature phenomenon. Certainly, for near-equilibrium behaviour, governed by quantum statistics, high temperatures make quantal effects less and less evident. But quantum information processing aims to stay far from equilibrium, and quantum dynamics can remain very important at higher temperatures. Practical issues may be serious, of course, as the approach to equilibrium may be fast.

A M Stoneham's group at University College London propose a new approach to constructing gates for quantum information processing, exploiting the properties of impurities in silicon. Quantum information, embodied in electron spins bound to deep donors, is coupled via optically induced electronic excitation. Gates are manipulated by magnetic fields and optical light pulses; individual gates are addressed by exploiting spatial and spectroscopic selectivity. These qubits are distributed in space such that mutual interactions are small in the normal (ground) state, in which they are able to store quantum information. In an electronic excited state, however, entangling interactions between qubits can occur. Only in excited states are pairs of qubits manipulated. Their approach therefore relies on knowing the natures of the excited states and on engineering the system so as to optimize these states. Such quantum gates do not rely on small energy scales for operation, so might function at or near room temperature. They show the scheme can produce the classes of gates necessary to construct a universal quantum computer.

Nanoscale cracks in glass

Crack fronts and damage in glass at the nanometre scale

Christian Marlière, Silke Prades, Fabrice Célarié, Davy Dalmas, Daniel Bonamy, Claude Guillot and Élisabeth Bouchaud

J. Phys.: Condens. Matter
15 No 31 (13 August 2003) S2377–S2386

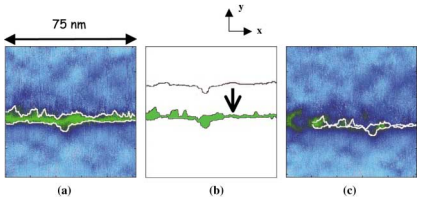

Fracture surface topography analysis (FRASTA). (a) Frame for broken sample is binarized and the contours of the crack are determined. (b) The lower line is first numerically raised over the upper one and then gradually displaced in the direction of decreasing y, as indicated by the arrow. Cavities are coloured in green. (c) Result of the method: superimposition of the obtained cavities on the image recorded prior to complete failure.

Materials fracture exhibits many puzzling aspects. It is especially hard to reconcile two different observations. Brittle materials (glass is a common example) break abruptly, without first deforming, whereas large plastic deformations precede fracture in ductile materials (like most metal alloys). In ductile fracture, the crack progresses through the coalescence of micrometric damage cavities nucleated from microstructural defects (second phase precipitates, grain boundaries . . .). Yet quantitative studies show both types of fracture surfaces to have a very similar morphology. Fracture surfaces are self-affine objects both for brittle and for ductile materials. Two self-affine regimes coexist: at small length scales (up to a length V_C), the roughness exponent N is close to 0.5 for length scales below a characteristic length V_C, whereas N is around 0.8 for larger length scales, up to a length V. These values of N are universal, but V_C and V depend on the kind of material considered. Values range from a few nanometers for glass to a few centimetres for concrete and rocks. For ductile materials, V_C is of the order of the typical size of the damage cavities when they coalesce. This strongly suggests that the observed transition between the two self-affine regimes reflects a change from an intra-cavity structure to an inter-cavity one.

A natural supposition is that there might be an undetected ductile-like fracture process in brittle materials like glass. If so, the size of the associated damage cavities at coalescence would be comparable with the crossover length V_C, of order 10 nm. Groups headed by C Marlière at Montpellier and E Bouchaud at Saclay sought to observe such an effect experimentally using atomic force microscopy. Huge velocity fluctuations in the progression of the tip were detected and explained by the observation of nanometric cavities developing ahead of the crack tip. That these were damage cavities was confirmed by using two independent methods. Their results confirm the scenario previously proposed by Bouchaud et al to explain the origin of the two self-affine regimes observed on fracture surfaces. The fact that glass, even at temperatures far below the glass transition temperature T_g, joins the class of damageable materials should have important consequences. The design of structures using glass might be modified to take this behaviour into account, especially for slow crack propagation processes. The similarity between the damage modes of materials as different as glass and metallic alloys is an important clue to aid our understanding of the origin of some puzzling universal behaviour, and sheds new light on the basic physical mechanisms of fracture.

Microscopy of amorphous materials

A quantitative measure of medium-range order in amorphous materials from transmission electron micrographs

R K Dash, P M Voyles, J M Gibson, M M J Treacy and P Klebinski.

J. Phys.: Condens. Matter
15 No 31 (13 August 2003) S2425–S2435

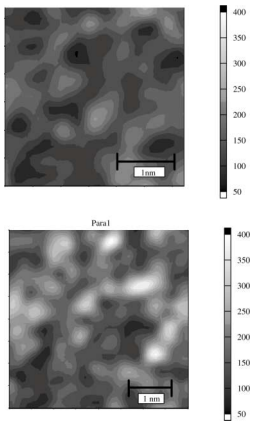

Grey scale contour plots of the calculated image intensity for the CRN and Para 1 structures. $Q = 0.056$ Å^{-1}, which is a real-space resolution of ~ 11 Å, $k = 0.56$ Å^{-1}, which is the position of the second maximum in S (k) for a-Si.

Understanding of the properties of amorphous and glassy materials has been hindered by incomplete knowledge of their atomic structure, especially beyond the shortest-range features. Diffraction experiments give the structure factor $S(k)$, and hence its Fourier transform $g_2(r)$, which gives the probability of finding two atoms in the sample separated by a distance r. But $g_2(r)$ is not very sensitive to medium-range order (MRO) present in many amorphous materials at the nm scale. Evidence for MRO comes from the anomalous first sharp diffraction peak found for many ionic and covalent glasses and from small-angle scattering. MRO is believed to affect diffusive, mechanical, optical and electronic properties of amorphous materials, such as the optoelectronic properties of amorphous silicon for solar-cell and flat panel display applications, known to deteriorate with exposure to light.

M M J Treacy (NEC, Princeton) and J M Gibson (Argonne) developed fluctuation electron microscopy (FEM) to provide more information about MRO in amorphous materials. FEM is the statistical analysis of fluctuations in diffraction from nanometre-scale volumes. Such local diffraction can be measured by transmission electron microscopy (TEM). Higher-order atomic distribution functions, more sensitive to medium-range structure than $g_2(r)$, contribute to FEM observations. Treacy and Gibson together with P M Voyles of University of Wisconsin, Madison and R K Dash and P Keblinski of Rensselaer Polytechnic Institute propose a new quantitative measure of MRO in amorphous materials, related to FEM. The spatial autocorrelation function of dark-field TEM image intensities shows an exponential decay. The decay length is determined by an intrinsic structural correlation length and the microscope resolution. The analysis indicates that measurements at a few discrete resolutions are sufficient to separate these effects and determine the intrinsic correlation length. This measure of MRO is demonstrated in simulated images from computer-generated models of a-Si and in experimental images of a-Si. The correlation length from the simulations follows the degree of medium-range order introduced a priori into the models. The correlation length in the experiments shows the same trend as previous FEM measurements for the same samples.

Laser modification of glass

Confocal fluorescence and Raman microscopy of femtosecond laser-modified fused silica

W Reichman, J W Chan and D M Krol

J. Phys.: Condens. Matter
15 No 31 (13 August 2003) S2447–S2456

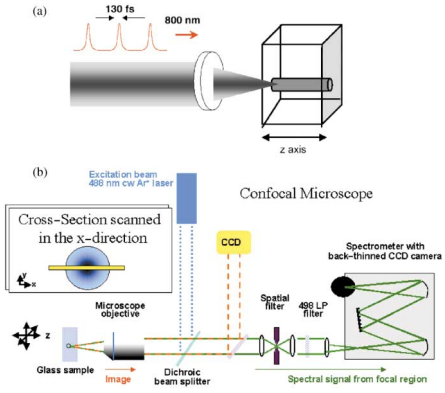

Schematic diagrams of (a) the experimental set-up for writing modified lines in fused silica with fs laser pulses and (b) the scanning confocal microscopy set-up used for fluorescence and Raman spectroscopy.

Femtosecond (fs) laser pulses — tightly focused inside a bulk glass — can induce localized refractive index changes of the glass within the focal volume of the laser beam. By scanning the glass with respect to the laser focus, waveguide structures can be fabricated inside the glass. This technique holds tremendous potential as a fabrication technique for three-dimensional all-optical integrated components with applications in telecommunications as well as in biological and chemical sensors and medical technology. The mechanism of ultrashort-laser-pulse modification of transparent materials can be divided into several steps. First, there is the production of initial seed electrons through either non-linear photoionization of free electrons or excitation of impurity defects. Avalanche photoionization follows, then plasma formation, and finally energy transfer from the plasma to the lattice so as to cause rebonding, or defect creation. This final step of energy transfer from the hot plasma created by the laser pulses to the lattice leads to modified regions in the bulk material with physical, chemical, and structural changes, such as densification, index increase, and/or colour centre formation, of the material after exposure to the laser beam.

In work by D M Krol's group at UC Davis and Lawrence Livermore, modified lines were written inside Corning 7940 fused silica with 130 fs laser pulses from an amplified Ti-sapphire laser operating at 800 nm at a repetition rate of 1 kHz. The sample was scanned at 20 μm s^{-1} with laser pulse energies ranging from 1 to 35 μJ, resulting in modified lines with diameters ranging from 8 to 40 μm. Confocal fluorescence and Raman microscopy probed for spatial variations in defect concentration and glass structure across the modified lines. The fluorescence intensity decreased with increasing distance from the line centre, whereas the Raman intensity increased. Contrary to previous work, no significant variations in the concentration of three- and four-membered ring structures were observed.

Magnetism in monatomic metal wires

P Gambardella

J. Phys.: Condens. Matter
15 No 34 (3 September 2003) S2533–S2546

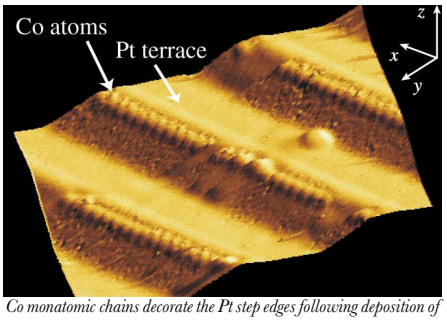

Co monatomic chains decorate the Pt step edges following deposition of 0.07 ML Co at T = 250 K (the vertical scale has been enhanced for better rendering). The chains are linearly aligned and have a spacing equal to the terrace width. The protrusion on the terrace is attributed to Co atoms incorporated in the Pt layer.

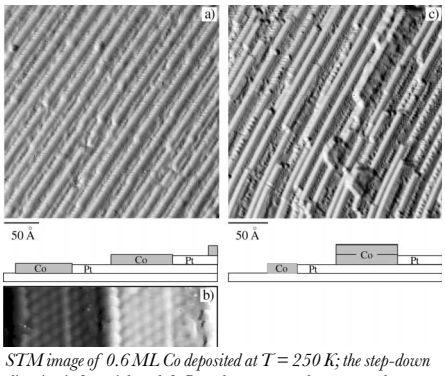

STM image of 0.6 ML Co deposited at T = 250 K; the step-down direction is from right to left. Row-by-row growth conserves the original step pattern. (b) Detail of two adjacent terraces with atomic resolution on the Co chains and Pt substrate.

P Gambardella of EPF Lausanne reported the first investigation of magnetism in one-dimensional (1D) monatomic chains of metal atoms. Gambardella and colleagues have used the surface of platinum oriented so as to present flat portions separated by regularly spaced steps. Cobalt is brought onto the surface in tiny amounts by evaporation. This fabrication process results in a very large number of regularly spaced straight Co chains glued to the edges of the Pt steps.

According to well-established theory of Mermin and Wagner (MW), a 1D atomic chain cannot possess any long-range magnetic order at non-zero temperature, but the measurements of Gambardella et al show that a ferromagnetic state can be reached below about 15 K thanks to the giant magnetic anisotropy energy (MAE) of the chains.

In the MW theory the chains are assumed to be infinitely long, whereas the experimental chains are finite. Gambardella argues that finite chains could be stable magnets on a temperature-dependent timescale. He also argues that the giant MAE, which is not part of the Heisenberg model considered by MW, stabilizes the 1D magnet.

The measurements by Gambardella and colleagues already initiated new theoretical work that led to an improved understanding of the experimental results. But many problems remain, especially as regards a detailed understanding of the giant MAE together with the finite-temperature problems of the magnetic nanowires.

This work provides a deeper understanding of 1D magnetism. Moreover, it shows that giant MAE can be obtained by artificially reducing the coordination of the magnetic atoms in surface-supported nanostructures, a key issue to design ever smaller magnetic bits in data storage devices.

Ferroelectric capacitor arrays

Self-patterning of arrays of ferroelectric capacitors: description by theory of substrate mediated strain interactions

M Dawber, I Szafraniak, M Alexe and J F Scott

J. Phys.: Condens. Matter
15 No 44 (12 November 2003) L667–L671

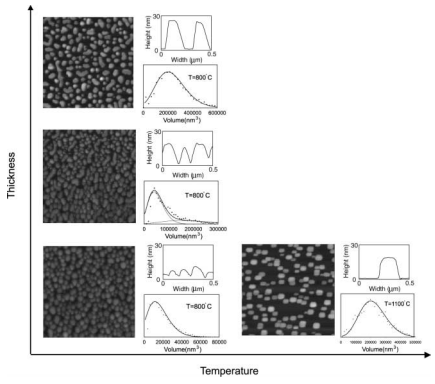

AFM images (size: 2.5×2.5 μm), profiles and volume distributions of PZT nanocrystals on $SrTiO_3$ for different dilution levels and temperatures. At 800 °C there is a transition from superdomes to domes as the dilution is increased (decreasing PZT thickness). Surprisingly at higher temperatures the most dilute film forms superdomes contrary to our expectation based on the results for Ge on Si(100).

Achieving higher density arrays of ferroelectric capacitors in a cost and time effective manner would be of great technological significance. One approach is to attempt to produce self-patterned arrays of nanocrystals, in which ordering is produced by interactions between islands through the substrate. This approach could be used to produce arrays of metallic nanoelectrodes on top of a ferroelectric film or, alternatively, arrays of crystals from the ferroelectric materials themselves.

J F Scott's group at Cambridge with co-workers from MPI for Microstructure Physics, Halle examined the structures formed in two cases, metallic bismuth oxide on bismuth titanate and ferroelectric lead zirconate titanate on strontium titanate.

They showed that the mechanism is the same as that evident in the formation of Ge islands on Si, for which a great deal of theoretical and experimental literature is available because they have been used to fabricate semiconductor quantum dots. A better understanding of the mechanism of formation of self-patterning ferroelectric nanocrystals should permit improved registration and regularity of crystal size by choice of materials and processing conditions. Their general conclusion, however, is that highly registered memory arrays will not occur spontaneously in the absence of a pre-patterned field.

Pettifor maps

Automatic construction, implementation and assessment of Pettifor maps

Dane Morgan, John Rodgers and Gerbrand Ceder

J. Phys.: Condens. Matter
15 No 25 (2 July 2003) 4361–4369

Predicting the stable crystal structures for materials is an important unsolved problem in materials science. First-principles approaches are limited by the time it takes to explore the many possible structures for a new system.

A well known, and remarkably simple, heuristic scheme is the 'Pettifor map', which assigns a numerical 'Chemical Scale' value to each element, allowing binary alloys A_xB_y to be mapped on Cartesian axes of the Chemical Scales for elements A and B. Alloys with similar stable structures will cluster together in the map, so the unknown stable structure for a new alloy system can be predicted by examining the stable structures of its nearby neighbours.

Dane Morgan's group at MIT have developed a method to automate the construction and testing of Pettifor maps based on data from a standard materials crystal structure database. They describe in detail the cleaning of the database entries — an essential step. They propose a nearest-neighbour method, which makes more accurate predictions than a dominant-neighbour approach. They confirm that the clustering properties of the Pettifor map greatly increase the predictive accuracy over a more naive approach based on the most frequently appearing structures. They show that generating a candidate structure list for predicting a new structure adds significant predictive accuracy to the Pettifor maps compared to just predicting a single structure. Using a cross-validation approach they show that the predictive accuracy of Pettifor maps for the AB and A_3B alloys is about 86% for a candidate list of five structures. Without unrepeated structures this predictive accuracy increases to 95%, demonstrating that there is only marginal room for improvement with data-mining methods that are restricted to predicting experimentally known structures. It is now possible to implement the automated construction, use and testing of Pettifor maps in materials databases, giving the opportunity to develop Pettifor maps in new alloy spaces quickly and easily.

Note: The maps can be accessed from http://www.tothcanada.com/PettiforMaps/

Quantum condensation of liquid ^{4}He

Mark Brown and Adrian F G Wyatt
J. Phys.: Condens. Matter
15 No 27 (16 July 2003) 4717–4738

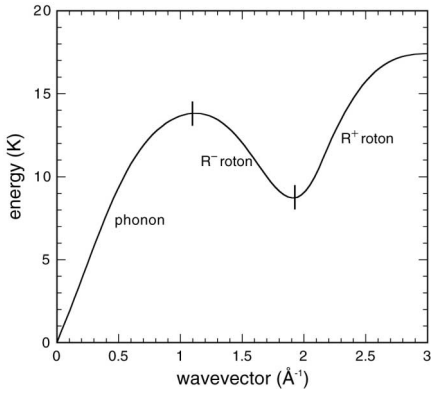

The dispersion curve for liquid ^{4}He showing the phonon, R$^-$ roton and R$^+$ roton regions.

Atoms in liquid ^{4}He form a Bose–Einstein condensate (BEC). In quantum evaporation, an atom in the condensate acquires sufficient energy to overcome the binding energy, from an excitation in the liquid. Mark Brown and Adrian Wyatt at Exeter describe the inverse process in which a ^{4}He atom condenses onto the free surface of liquid ^{4}He and produces an excitation in the liquid.

There are three types of excitations - phonons and two types of rotons: R$^+$ and R$^-$ with positive and negative group velocity respectively. It is known that all three can cause quantum evaporation: high-energy phonons and R$^+$ rotons readily eject ^{4}He atoms from the surface of liquid ^{4}He, but R$^-$ rotons create free atoms with a much lower probability. The present experiments show that both phonons and R$^+$ rotons are created in one-to-one processes, with conservation of energy and parallel momentum. There is no detectable signal due to R$^-$ rotons, showing the probability for this channel is very low. The experiments also give the first clear evidence that R$^+$ rotons can be directly detected.

Surface excitations, known as ripplons, are the most likely excitations to be produced by condensing atoms. The created ripplons decay by producing phonons, which can be distinguished from the quantum-condensation phonons.

Just as quantum evaporation has enabled the study of ballistic high-energy phonons and rotons, so too quantum condensation promises to further the study of roton–roton interactions. The high flux of R$^+$ rotons produced by condensation will enable new scattering experiments to be done.

The most important conclusion from these experiments is that quantum condensation, the time-reverse of quantum evaporation, exists.

'Hot' spin ice

Dynamical crossover in 'hot' spin ice
G Ehlers, A L Cornelius, M Orendác, M Kajnaková, T Fennell, S T Bramwell and J S Gardner
J. Phys.: Condens. Matter
15 No 2 (22 January 2003) L9–L15

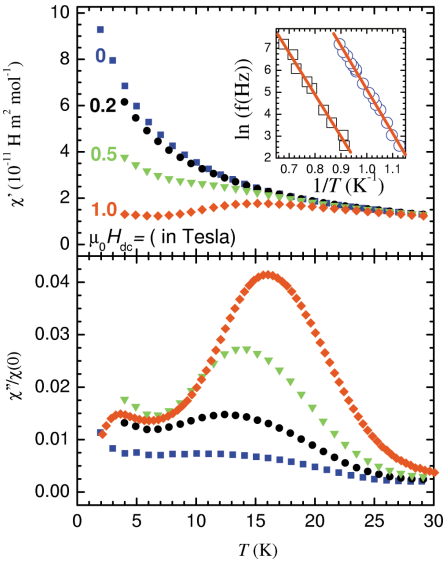

AC susceptibility results for $Ho_2Ti_2O_7$, measured with a field of 1 T along [111], revealing a peak ~ 15 K. Inset shows an Arrhenius plot for the frequency shift of the ~ 1 K peak in polycrystalline $Ho_2Ti_2O_2$ (squares) and $Ho_{1.9}La_{0.1}Ti_2O_7$ (circles) showing how doping increases the attempt frequency for the lower temperature process.

In materials such as $LiHoF_4$, in which the spin is confined to a double-well potential of depth D arising from the crystalline electric field, quasiclassical spin reorientations are precluded at temperatures $T \ll D/k_B$, but spin relaxation may still occur. Direct transitions of this sort, between degenerate $|\pm M_J\rangle$ states on either side of the barrier, are referred to as 'spin tunnelling'.

In the 'spin ice' materials $Ho_2Ti_2O_2$, $Dy_2Ti_2O_7$, and $Ho_2Sn_2O_7$, $D/k_B > 200$ K is much larger than in other magnets. The spins are constrained to local axes, which leads to frozen, non-collinear, spin disorder below ~1K.

S T Bramwell of University College London, J S Gardner at NIST and co-workers have isolated the spectral properties of spin-ice materials and, where possible, identified their origin using the elegant technique of neutron spin echo, which involves a beam of spin-polarized neutrons executing a fixed number (say N) of spin precessions prior to striking the sample. The sense of the precession is then reversed by static magnetic fields near to the sample position. After N further precessions the original polarization is restored, unless scattering processes in the sample have produced a phase shift.

In conclusion, $Ho_2Ti_2O_7$ presents a very different scenario to other quantum magnets, as here the tunnelling dynamics are an intrinsic consequence of the geometric frustration that prevents magnetic ordering. Cooperative quantum tunnelling occurs over a broad range of unusually high temperatures, from $T \approx 1$–15 K, while a single-ion process dominates above 15 K. The authors have elucidated the main relaxation processes in the 'hot' paramagnetic phase of $Ho_2Ti_2O_7$ and the other spin ices, which they believe may represent a remarkable new class of quantum dynamical magnet.

Magnetism of metal clusters

On the oscillation of the magnetic moment of free transition metal clusters
Yuannan Xie and John A Blackman
J. Phys.: Condens. Matter
15 No 40 (15 October 2003) L615–L622

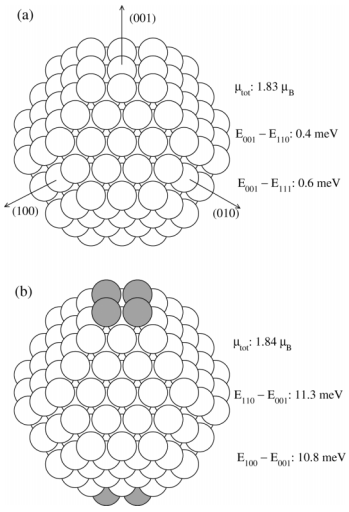

Total average magnetic moments μ_{tot} and MAEs calculated from TB models for (a) Co_{201} and (b) Co_{209}. Co_{209} is constructed from Co_{201} by adding one layer (shadowed atoms) to the top and bottom squares.

A better understanding of magnetism in transition metal clusters is crucial not only for fundamental physics but also for potential applications in high-density data storage devices.

The results of Stern–Gerlach experiments on free clusters of Fe, Co, and Ni are usually interpreted in terms of magnetic moments that show oscillations as a function of cluster size. Yuannan Xie and John Blackman of Reading have shown that the observed behaviour can be more convincingly explained in terms of magnetic anisotropy energies (MAEs) that oscillate with the size of the clusters.

The MAE, i.e. the energy involved in rotating the magnetization from a low energy direction (easy axis) to a high energy direction (hard axis), determines the low temperature orientation of the magnetization with respect to the structure of the system. The MAEs of clusters are higher than the bulk values because of a strong anisotropy induced at the surface of the clusters.

They show that the apparent oscillations of the magnetic moments present in the experiments on free clusters can be properly analysed by taking the MAE into account. The MAEs of free Fe, Co, and Ni clusters are estimated under various reasonable experimental conditions and theoretical postulates. The estimated MAEs are in reasonably good agreement with the experimental results for supported/embedded cluster assemblies, which verifies the validity of their theoretical model.

Photonic minibands

Appearance of photonic minibands in disordered photonic crystals
M A Kaliteevski, J Manzanares Martinez, D Cassagne, J P Albert, S Brand and R A Abram
J. Phys.: Condens. Matter
15 No 6 (19 February 2003) 785–790

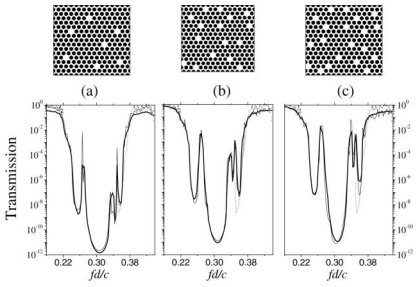

(a) Transmission spectra for the supercell with a single vacancy (dotted curve). (b) Transmission spectra for photonic supercrystal PSC1 (solid curve). (c) Transmission spectra for photonic supercrystal PSC2 (solid curve). The transmission spectra of the ideal structure (dashed curve) and supercell with the single vacancy (dotted curve) are shown on all figures for comparison.

Photonic crystals have potential applications in optoelectronics but fabrication-related disorder prevents their widespread use. R A Abram's group at Durham with co-workers at Montpellier investigated the influence of random or ordered configurations of vacancies in a photonic crystalline lattice on its optical properties and density of modes. They considered two-dimensional photonic crystals with defects in the form of either an ordered periodic or a random distribution of vacancies. In both cases they showed the presence of photonic minibands within the photonic bandgaps. The positions of the minibands are defined by the energies of the localized photonic states of the single defect, and their width increases with increase in the concentration of the defects. The appearance of these minibands makes it possible to construct suitably engineered photonic microstructures to produce spectral filters with thin transmission bands.

Polarons in high-T_c superconductors

Signatures of mesoscopic Jahn–Teller polaron inhomogeneities in high-temperature superconductors
A R Bishop, D Mihailovic and J Mustre de León
J. Phys.: Condens. Matter
15 No 9 (12 March 2003) L169–L175

Recent experimental results have suggested the onset of an inhomogeneous ground state for the doped cuprates as a precursor to the superconducting phase and theoretical models have been developed to explain it.

A R Bishop at Los Alamos and co-workers connect such experimental results with the predictions of quantum mechanical calculations of small polaron formation and internal dynamics (phonon-assisted local charge oscillations). This provides evidence that in high-T_c cuprates T^*, the so-called pseudogap temperature, marks the onset of polaron formation and there is a change in the dynamics of these polarons across the superconducting transition temperature, T_c, suggesting their relation to the mechanism of high-temperature superconductivity.

The theoretical models treat small Jahn–Teller (JT) polarons, which involve coupling of specific in-plane and axial copper–oxygen vibrations to charge carriers. Below T^* the individual polarons become thermally stable, forming a polaron liquid of filamentary segments with at most a very slow polaronic diffusion, but with a much faster internal charge tunnelling accompanied by dynamic lattice distortions — a fundamentally quantum mechanical effect – leading to an internal dynamical symmetry breaking. This phenomenon is also present in other organic and inorganic systems. Predicted consequences of the existence of small JT polarons have been observed experimentally. The data currently are evidence for small polarons and do not distinguish isolated polarons from their anticipated organization into filamentary segments for $T^* > T > T_c$ as precursors to correlated percolation paths for $T < T_c$.

The substantial semi-quantitative consistency among all the different data analysed here strongly suggests the need for new, more extensive systematic experimental studies, which can be compared quantitatively with theoretical predictions, and hopefully reveal the detailed connection between these effects and superconductivity in cuprates.

Self-organized criticality in friction

Evidence of self-organized criticality in dry sliding friction
Fredy R Zypman, John Ferrante, Mark Jansen, Kathleen Scanlon and Phillip Abel
J. Phys.: Condens. Matter
15 No 12 (2 April 2003) L191–L196

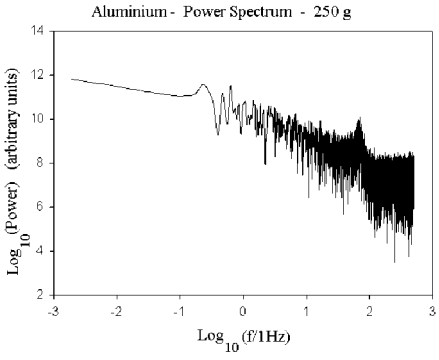

Frequency power spectrum of the original data for aluminium at 250 g load.

The classic example of self-organized criticality (SOC) is a sandpile to which grains are continuously added at its apex. When the slope of the pile reaches a threshold angle, a critical state, energy is released through avalanches that keep the angle constant. Stick – slip friction shows similar behaviour.

SOC is characterized by power-law slip sizes distribution, a $1/f$ frequency power spectrum, and the presence of a stationary state, evidence of an attractor defining the critical state. Fredy Zypman of Yeshiva University, J Ferrante and co-workers at NASA-Glenn Research Center examined stick–slip in dry friction using a pin-on-disc tribometer. They examined the probability distributions of slip sizes for matching aluminium and M50 steel pins and discs for evidence of SOC.

They found that pin-on-disc, dry sliding stick–slip satisfies the two most important characteristics for SOC. Is stick–slip in dry friction therefore an example of SOC? The number of states in the system may not be large enough for self-organization, since the number of asperities making a contact is assumed to be a few hundred. However, recent microscopic studies show stick–slip behaviour even in the presence of a single asperity, which suggests that microasperities may be the determining mechanism, so a smaller scale may be dominant. Whatever the mechanism, friction has its origin at a microscopic level, where a large number of atoms play a role.

At this point they cannot offer a microscopic theoretical model, since there are no such accepted models for either friction or SOC. To the extent that SOC and dry friction are understood today, stick–slip in dry friction behaves as a SOC system. This study implies the clear need for further research into SOC in tribology.

Photoluminescence in mesoporous nanotubes

Blue–green photoluminescence in MCM-41 mesoporous nanotubes
Finlay D Morrison, Laura Ramsay and James F Scott
J. Phys.: Condens. Matter
15 No 20 (28 May 2003) L297–L304

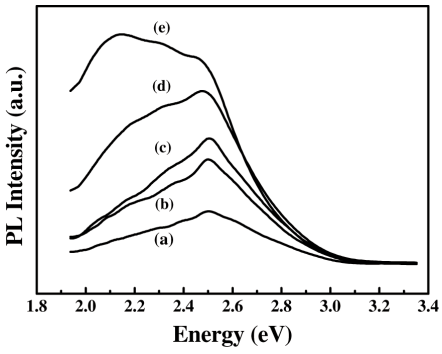

PL spectrum of MCM-41 as-synthesized (a) and after RTA at 200 °C (b), 400 °C (c), 600 °C (d), 800 °C (e).

Mesoporous siliceous M41S materials are important because of their high pore volume, large surface area, and very narrow pore-size distribution. They have potential applications in heterogeneous catalysis, photocatalysis, adsorption, gas separation, and ion exchange. It is useful to study their optical properties to clarify the nature of the structural defects, and provide useful information for applications in optical devices. The red photoluminescence (PL) of MCM-41is attributed to oxygen-related defects, but several models have been proposed for the origin of the blue–green PL. J L Shen and co-workers from Chung Yuan Christian University, Taiwan have tried to clarify the origin of the blue–green PL in MCM-41 nanotubes using different PL techniques.

They found that the intensity of blue–green PL was enhanced by rapid thermal annealing treatment, suggesting potential applications in light-emitting and optical memory devices. They explained this enhancement by the generation of twofold-coordinated Si centres and non-bridging oxygen hole centres in line with the surface properties of MCM-41. Through the analysis of polarized PL, they found the blue–green PL centres are anisotropic with a degree of polarization of 0.25. They also performed the first PL excitation studies of MCM-41, finding a main excitation band of blue–green emission at 3.47 eV. These PL studies strongly suggest that the blue–green PL in MCM-41 nanotubes is due to a triplet-to-singlet transition of twofold-coordinated silicon centres. The studies presented here are expected to be useful for clarifying the nature of light emission in MCM-41 and to be of practical use for possible applications in optical devices and as a photocatalyst.

Ferroelectric nanotubes

High aspect ratio piezoelectric stronium-bismuth-tantalate nanotubes
J L Shen, Y C Lee, Y L Lui, P W Cheng and C F Cheng
J. Phys.: Condens. Matter
15 No 33 (27 August 2003) L527–L532

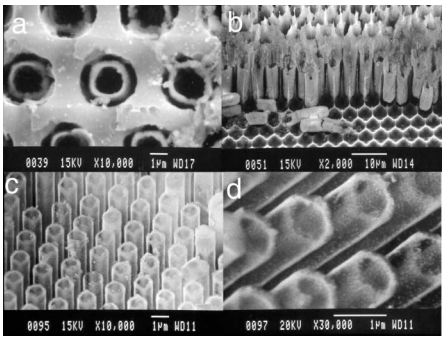

Schematic diagram of the molecular field within Fe clusters adsorbed on vitrovac due to the exchange interaction at the contact point between the clusters and the substrate.

Ferroelectric nanotubes made of oxide insulators have applications in pyroelectric detectors, piezoelectric ink-jet printers, and memory capacitors. To increase the storage density in FRAM and DRAM devices, complicated stacking geometries, 3D structures, and trenches with high aspect ratios so as to increase the dielectric surface area are being investigated. J F Scott's group at Cambridge have reported the integration of ferroelectric nanotubes into Si substrates, which is particularly important in construction of 3D memory devices.

Template synthesis of nanotubes and wires enables the size, shape, and structural properties of the assembly to be simply controlled. Using carbon nanotubes as templates, tubular forms of a number of oxides have been generated. Much larger (>20μm diameter) ferroelectric microtubes have been made by sputter deposition around polyester fibres.

Using porous photonic Si crystals with a regular array of pores of diameter 400 nm to a few microns and 100 μm deep as templates, they have successfully produced uniform coatings of ferroelectric $SrBi_2Ta_2O_9$ <100 nm thick with high aspect ratios. On partial removal of the Si template, it is possible to produce a periodic array of nanotubes in which each tube is completely discrete. This is in contrast to other template approaches, which produce either individual, free-standing nanotubes or 'bundled' or entangled structures. The formation of a periodic array has several advantages in terms of addressing/registration for device applications. It is envisioned that oxide nanotubes can be used in fluidic devices for analysis and control of molecular species, nanoelectronic devices, catalysis, and nanoscale delivery vehicles. The very large surface/volume ratio makes catalytic devices particularly attractive. Piezoelectric and ferroelectric nanotubes of SBT therefore have potential for a variety of applications in addition to those in ferroelectric memory devices.

Landauer formula without Landauer's assumptions

Mukunda P Das and Frederick Green
J. Phys.: Condens. Matter
15 No 45 (19 November 2003) L687–L693

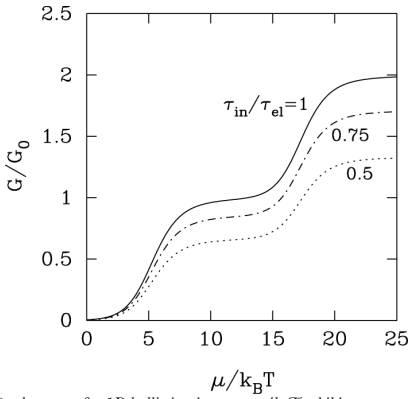

Conductance of a 1D ballistic wire versus μ/k_BT exhibits strong shoulders as μ crosses the sub-band energy thresholds at 5 and 17 k_BT. Well above each threshold, sub-band electrons are strongly degenerate and the conductance tends to a plateau. Full curve: ballistic channel, ideal limit $\tau_{in}/\tau_{el} = 1$; chain curve: non-ideal case $\tau_{in}/\tau_{el} = 0.75$; dotted curve: $\tau_{in}/\tau_{el} = 0.5$. Note how the increased inelastic scattering brings down the plateaux.

Rolf Landauer's classic interpretation of metallic resistivity predicted the perfect quantization, in steps of $2e^2/h$, of electrical conductance in one-dimensional metallic channels. His formula assumes that there are no inelastic processes to dissipate the electrical energy gained by the electrons. Yet it is dissipative inelastic scattering that ensures the energetic stability of resistive transport and hence a steady state for conduction. Finite conductance and electrical energy loss are indivisible phenomena, as expressed by the fluctuation-dissipation theorem (FTD).

Mukunda Das and Frederick Green of Australian National University, have answered the question: how can the Landauer formula, in seemingly bypassing all inelastic processes, predict a finite—invariably dissipative—conductance that fulfils the FDT? They show that the traditional Landauer assumptions of pseudo-diffusive current and lossless scattering are not required. The model relies solely upon the orthodox quantum kinetics of the microscopic Kubo–Greenwood formalism, which automatically guarantees the FDT. Both dissipative and lossless scattering appear within the resulting fluctuation–dissipation relation and both are assigned equal physical importance.

They show how the Landauer conductance formula arises directly from a fine-scale interplay of elastic and inelastic processes in one-dimensional ballistic conductors, thus automatically respecting charge conservation and the FDT.

The Landauer theory's traditional phenomenological assumptions are not required for the validity of the formula itself, provided the essential physics of resistive energy dissipation is respected. A minimal set of assumptions not only recovers the full Landauer formula, but also reveals considerably more information.

In a mesoscopic ballistic conductor open to its electrical environment, the close interaction between dissipative and elastic scattering uniquely governs the behaviour of the conductance. Neither of the collision modes, acting alone, can sustain the physics of mesoscopic transport. A theory of transport must allow all such processes to act in concert.

Encapsulated magnetite particles for biomedical application

Katharina Landfester and Liliana P Ramírez
J. Phys.: Condens. Matter
15 No 15 (23 April 2003) S1345–S1361

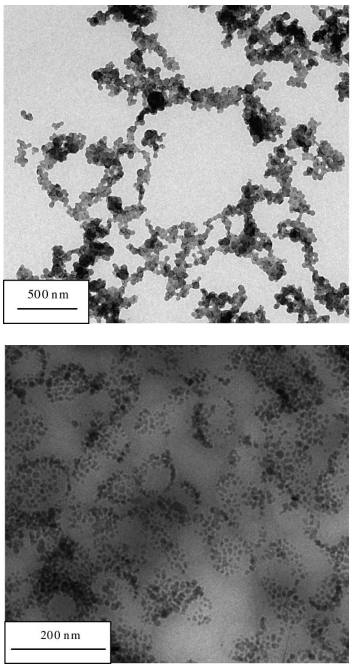

TEM images for magnetite polystyrene particles at different magnifications.

Particles composed of polymers or hybrid polymeric and magnetic materials have important biomedical applications, for which they need to be biocompatible and non-toxic, and sometimes also biodegradable. Many different approaches are used to produce nanoparticles with these properties.

Katharina Landfester and Liliana P Ramírez of MPI of Colloids and Interfaces, Potsdam, have demonstrated the possibility of using the miniemulsion process for formulation of magnetic nanoparticles. The encapsulation of large numbers of magnetite particles into polystyrene particles can be achieved efficiently by a new three-step preparation route including two miniemulsion processes. First, oleic-acid-coated magnetite particles in octane are prepared. Secondly, a dispersion of the magnetite in octane is miniemulsified in water by using SDS as the surfactant. After evaporation of the octane, the magnetite aggregates which are covered by an oleic acid/SDS bilayer are mixed with a monomer miniemulsion and, in the third step, an ad-miniemulsification process is used to obtain final and full encapsulation. Here, a fusion/fission process induced by ultrasound is only effective for the monomer droplets, whereas the monomer-coated magnetite aggregates remain intact. In that way, all monomer droplets are split and heteronucleated onto the magnetite aggregates to form a monomer film. After polymerization, polymer-encapsulated magnetite aggregates were obtained. Characterization by thermogravimetry, preparative ultracentrifugation and transmission electron microscopy showed that up to 40% magnetite could be encapsulated, resulting in particles with a high homogeneity of the magnetite content.

Magnetometry measurements reveal that the magnetite aggregates still consist of separated superparamagnetic magnetite particles, which is due to the coverage by the oleic acid. During the encapsulation process, 60% of the magnetization compared to bulk magnetite is preserved.

Self-trapped states in proteins?

Robert H Austin, Aihua Xie, Lex van der Meer, Michelle Shinn and George Neil
J. Phys.: Condens. Matter
15 No 18 (14 May 2003) S1693–S1698

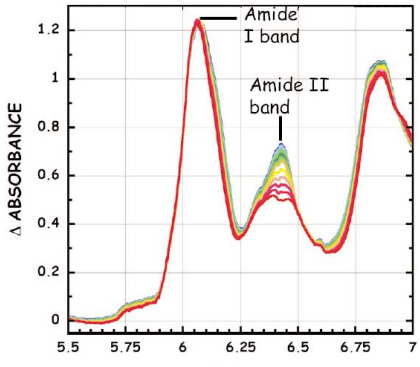

Temperature dependence of sperm whale MB (swMB) in the region 1800–1400 cm^{-1}. The colours of the curves are spectrally coded to correspond to temperature, with red = 300 K, yellow = 180 K and blue = 5 K.

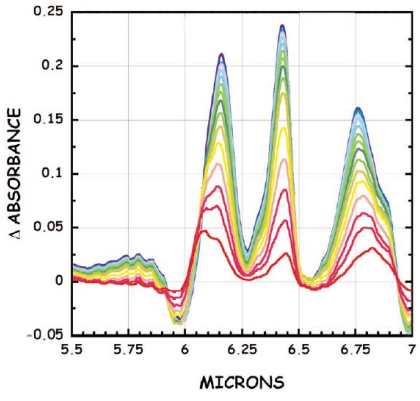

Difference spectra taken from the figure above, using the same colour scheme to plot difference between absorbance at temperature T and at 300 K.

Energy and charge transport are crucial to life. How can the energy from light or chemical processes be moved around and used efficiently at normal temperatures? In the 1970s, Davydov suggested that solitons provided an effective mechanism for energy transfer in proteins. Verifying this has proved difficult, for it is hard to identify a 'smoking gun' to be sure of an identification.

Robert Austin (Princeton) and his co-workers have found that experiments exploiting the short, turnable pulses from free-electron lasers appear to resolve some of the key questions. The temperature dependence of the amide I band of myoglobin shows evidence for a low-lying self-trapped state at 6.15μm. Careful picosecond pump-probe experiments as a function of temperature and wavelength show that this low-lying state has a 30 ps lifetime at 50 K, much longer than the relaxation time of the main amide I band at 50 K. A fit of the temperature dependence indicates that it lies 280 K below the main amide I band.

Since the gap energy of this state is of the order of room temperature, this self-trapped state can act as a transient store of vibrational energy at physiological temperatures in biomolecules, and can help to direct the path of energy flow in a biomolecule under biological conditions.

A new superconductor

Superconductivity in a pyrochlore-related oxide KOs_2O_6

S Yonezawa, Y Muraoka, Y Matsushita and Z Hiroi
J. Phys.: Condens. Matter
16 No 3 (28 January 2004) L9-L12

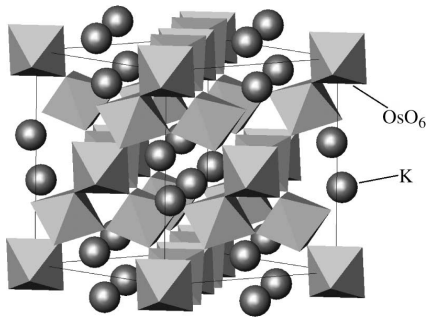

Probable crystal structure for KOs_2O_6. K, Os and O atoms occupy the 8b, 16c and 48f sites in the space group $Fd\bar{3}m$, respectively.

Pyrochlore oxides have a general chemical formula $A_2B_2O_7$ or $A_2B_2O_6'$, where A is a larger cation and B is a smaller transition metal (TM) cation. Most pyrochlore oxides containing 5d TM elements such as Re, Os and Ir are bad metals. Recently, superconductivity was found for the first time in a pyrochlore oxide in $Cd_2Re_2O_7$ at $T_c = 1$ K. A related pyrochlore oxide $Cd_2Os_2O_7$ undergoes a metal–insulator (MI) transition at 225 K. The major difference between them seems to be the number of d electrons on the B-site cations: Re^{5+} being $5d^2$ and Os^{5+} $5d^3$.

S Yonezawa's group from Tokyo have reported the discovery of superconductivity in a new ternary phase KOs_2O_6. Polycrystalline samples were prepared from KO_2 and OsO_2 powders. Resistivity measurements showed a superconducting transition with onset temperature 9.9 K and zero resistivity below 9.0 K. When a magnetic field was applied, the transition curve shifted to lower temperatures systematically. The resistivity above the transition shows a peculiar temperature dependence, which is far from that of a conventional metal. Measurements on a single crystal instead of a polycrystalline pellet are needed to clarify this point. The sample also showed a Meissner effect below 9.6 K. The superconducting volume fraction estimated at 2 K from the zero-field cooling experiment is about 80%, which is large enough to constitute bulk superconductivity.

They believe that an interesting physical process is involved in this compound on the basis of electron correlations near the MI transition as well as frustration on the pyrochlore lattice

REVIEWS

Mesomagnetism

The defining length scales of mesomagnetism: a review

C L Dennis, R P Borges, L D Buda, U Ebels, J F Gregg, M Hehn, E Jouguelet, K Ounadjela, I Petej, I L Prejbeanu and M J Thornton

J. Phys.: Condens. Matter
14 No 49 (16 December 2002) R1175–R1262

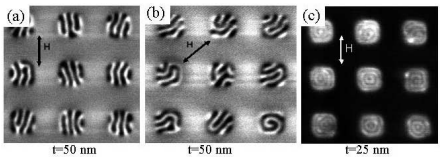

Example of stripe domains induced in ~ 0.5 μm wide epitaxial Co(0001) dots 50 nm thick and demagnetized (a) parallel to the edge of the square dot and (b) along the diagonal. (A change in domain orientation in an MFM image is indicated by a change from white to black.) (c) Circular stripe domains induced in ~ 0.5 μm wide epitaxial Co(0001) dots 25 nm thick and demagnetized parallel to the edge of the square dot.

Mesomagnetism is the study of the novel physical phenomena which appear when magnetic systems are reduced to the nanoscale. Magnetic processes are characterized by specific length scales and when the physical size of a magnetic system is engineered to these or smaller dimensions, novel behaviour is observed. Examples include giant magnetoresistance (GMR), Coulomb blockade, perpendicular anisotropy, superparamagnetism and current-induced switching.

As technology continues to miniaturize and novel materials are developed, these characteristic length scales and their resulting phenomena define the ultimate limits of devices. Many of these mesoscopic characteristic length scales— domain size, domain wall width, exchange length and thin film perpendicular anisotropy threshold—are governed by minimization of energy considerations. Others, like the spin diffusion length and spin precession length, are the result of diffusion processes for energy, momentum or magnetization. The phenomena that appear when magnetic systems are engineered on these length scales may be very diverse since a wide variety of combinations of several characteristic lengths may be involved.

These mesoscopic phenomena place ultimate limits on device performance, improve current technology or generate new technology. The electronics, data storage and computer industries and other industries including medical technology are continuously pushing the limits of technology. This has led to the development of novel devices (such as biological physics sensors for medicine) as well as advancements in GMR for read heads in data storage, the investigations into domains in granular media for data storage, magnetic field sensing for automotive sensors (and other applications which require sensors), MRAM and many others. Other investigations are pursuing more advanced concepts like single electronics for quantum computers.

A review by J F Gregg's group at Oxford and co-workers at IPCMS, Strasbourg, and Université Henri Poincaré, Nancy provides an introduction to mesomagnetism, exploring the connections between the different phenomena and their characteristic length scales as well as their relevance to (or operation in) devices.

Organic electronics

Organic–inorganic semiconductor devices and 3, 4, 9, 10 perylenetetracarboxylic dianhydride: an early history of organic electronics

S R Forrest

J. Phys.: Condens. Matter
15 No 38 (1 October 2003) S2599-S2610

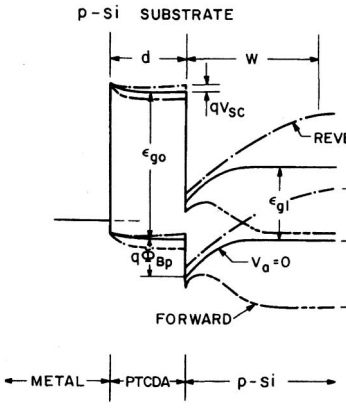

A proposed energy level diagram of a PTCDA/p-Si OI diode under equilibrium, and under forward and reverse bias.

The first organic-on-inorganic semiconductor heterojunction (OI HJ) was demonstrated in 1981, with the organic semiconductor 3, 4, 9, 10 perylenetetracarboxylic dianhydride (PTCDA), i.e. $C_{24}O_6H_8$.

S R Forrest of Princeton first investigated a test structure consisting of a metal contact and a 100–500 nm thick layer of PTCDA on a p-type Si substrate. It was expected to result in a simple metal–insulator–Si capacitor but, surprisingly, PTCDA formed a rectifying contact on Si, with nearly ideal characteristics. Both n- and p-type substrates, not only of Si but also of such materials as GaAs and InP, formed rectifying junctions with an organic semiconductor layer.

Forrest reviews possible applications of organic-inorganic heterojunction devices and describes the dramatic change in conductive properties of these materials when exposed to high-energy ion beams.

The prospects for hybrid organic-on-inorganic semiconductor structures for use in electronic and photonic applications are also presented, which include non-linear optical elements and even memory devices. While it remains to be seen which applications will emerge, the rapidly growing interest in organic electronics will almost certainly open a niche for OI HJ devices based on their very high performance and simplicity of fabrication.

Moreover, the extensive study of the remarkable, archetypal compound PTCDA has revealed much fundamental knowledge in the physics of organic semiconductors in general. Controlled OMBD growth has led to unprecedented film quality, which has allowed exploration of the spectroscopic and conductive properties of this material in films with ordered structures and of thicknesses from sub-monolayer to several microns. Analogues of PTCDA are showing promise for use in transistors, organic solar cells and photodetectors. Thus, the lessons learnt from this remarkable organic semiconductor will stimulate further rapid advances in organic electronics.

Nanostructures from nanoparticles

Paula M Mendes, Yu Chen, Richard E Palmer, Kirill Nikitin, Donald Fitzmaurice and Jon A Preece

J. Phys.: Condens. Matter
15 No 42 (29 October 2003) S3047–S3063

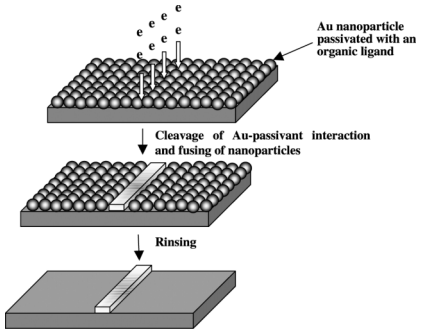

Fabrication of gold-based wires by electron beam writing in films of passivated gold nanoparticles.

Precise control of the structure of matter at the nanometre scale may have revolutionary consequences for science and technology. The ability to assemble nanoparticles into arrays, networks and circuits in a precise and controlled manner is the key to the fabrication of a variety of nanodevices. Networks of nanometre-sized metal or semiconductor islands, or quantum dots, may exhibit quantum phenomena, with potential applications in optical devices, nanometer-scale sensors, advanced computer architectures, ultra-dense memories and quantum information processing.

The fabrication of nanoparticle arrays with nanoscale precision remains a formidable task. Traditional semiconductor fabrication is based on 'top-down' techniques, i.e. lithography, and the construction of nanostructures by assembling molecular-sized components, but the so-called 'bottom-up' chemical approach may offer advantage including experimental simplicity down to the atomic size scale, the possibility of three-dimensional assembly and the potential for low-cost mass fabrication. Research in this field will help to understand how ordered or complex structures form spontaneously by self-assembly, and how such processes can be controlled in order to prepare structures with a pre-determined geometry.

Richard Palmer's group at Birmingham and Donald Fitzmaurice's group at University College Dublin review their progress in developing methods for producing nanostructures from metal nanoparticles. Three main approaches are discussed:

- formation of nanowires by direct electron beam writing in Au films passivated with organic ligands. Demonstrations of nanostructure fabrication by this method on practical Si/SiO_2 surfaces are also given.
- generation, or programmed assembly, of complex nanocrystal architectures in solution. Silver nanocrystals stabilized by a mixture of chemisorbed alkanethiol (85%) and similar molecules incorporating a molecular recognition group are shown to undergo chemical assembly.
- chemical modification of self-assembled monolayers by x-ray irradiation (nitro to amine group conversion), which promises to produce chemically patterned surfaces for selective nanoparticle attachment.

Together these three approaches represent a toolbox for the fabrication of novel nanometre scale architectures on surfaces.

Magnetism of films, stripes and dots

The effect of spatial confinement on magnetism: films, stripes and dots of Fe on Cu(111)
J Shen et al.
J. Phys.: Condens. Matter
15 No 2 (22 January 2003) R1-R30

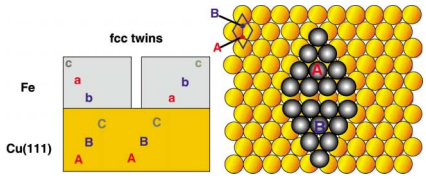

Schematics showing the phenomenon of twinning. The spacing between iron atoms on the Cu(111) surface is such that iron atoms in a particular island will either occupy 'A' sites only or 'B' sites only, depending on which of these two sites was settled upon by the atom that seeded the island. The image shows the fault line that forms when an A-type island tries to merge with a B-type island.

Magnetic nanostructures are important both for their basic physics and device applications. New properties that emerge at the nanoscale have at least four origins:

(1) Surface and interface effects dominate as the surface-to-volume ratio increases.

(2) New quantum phenomena such as oscillatory exchange coupling, GMR, spin-dependent tunnelling and exchange bias manifest in magnetic multilayers.

(3) Effects when the system dimensions are comparable with 'characteristic lengths' such as the spin-diffusion length — the exotic effects seen in GMR spin valves, for example.

(4) In many spin systems, like CMR materials and magnetic semiconductors, correlation effects spin fluctuations and spin transport, already important in the bulk spin structure, are enhanced by spatial confinement.

E W Plummer's group at Oak Ridge and J Kirschner at MPI for Microstructure physics, Halle review the successful growth of ultrathin films, nanowires and nanodots of Fe on Cu(111) using self-assembly principles, even though they cannot be grown by conventional techniques. The fact that these three types of nanostructures can be grown on a common template allows direct observation of the effects when the Fe nanostructures are smaller than the magnetic domain size in one, two and three dimensions. This particular system, Fe on Cu(111), has shown that the magnetic properties of a system do not change monotonically and predictably as the dimensionality of the system is reduced. Unresolved issues include the microscopic origin of the low-moment phase and the anomalous thickness dependence of the Curie temperature in laser MBE-grown films, and the surprising difference in the magnetic stability of the nanowire and quantum systems.

Future work on magnetic nanostructures prepared on insulating substrates, where there would be true confinement of the electrons, could be of particular importance. These systems might show, for instance, how electron spin can influence electronic transport in a magnetic nanowire. However, a considerable amount of work remains in developing techniques for the controlled synthesis of such systems.

Spin-dependent tunnelling

Spin-dependent tunnelling in magnetic tunnel junctions
Evgeny Y Tsymbal, Oleg N Mryasov and Patrick R LeClair
J. Phys.: Condens. Matter
15 No 4 (5 February 2003) R109–R142

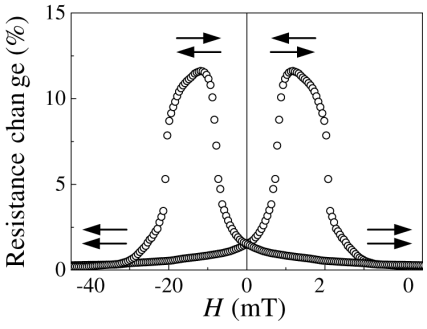

The first observation of reproducible, large room temperature magnetoresistance in a CoFe/Al_2O_3/Co MTJ. The arrows indicate the relative magnetization orientation in the CoFe and Co layers.

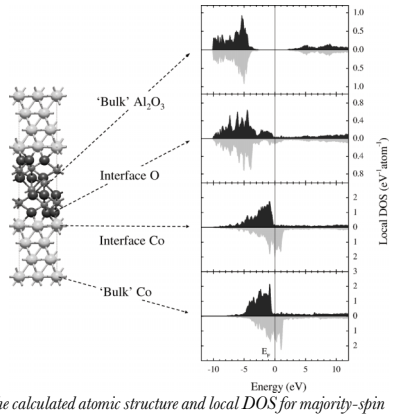

The calculated atomic structure and local DOS for majority-spin electrons (top panels) and minority-spin electrons (bottom panels) for a Co/Al_2O_3/Co tunnel junction.

A magnetic tunnel junction (MTJ) consists of two ferromagnetic metal films separated by an insulating barrier layer. The insulating layer is so thin (a few nanometres or less) that electrons can tunnel through the barrier if a bias voltage is applied. The tunnelling current depends on the relative orientation of the magnetizations of the two ferromagnetic films, which can be changed by an applied magnetic field — so-called tunnelling magnetoresistance (TMR).

MTJs based on 3d-metal ferromagnets and Al_2O_3 barriers can now be fabricated with reproducible characteristics and with TMR values up to 50% at room temperature, making them suitable for industrial applications. TMR is a consequence of spin-dependent tunnelling, which is an imbalance in the electric current carried by up- and down-spin electrons. The tunnelling spin polarization is not an intrinsic property of the ferromagnet alone but depends on the structural and electronic properties of the entire junction. This makes the quantitative description of transport characteristics of MTJs much more complicated, but broadens the possibilities for engineering the properties of MTJs for device applications. The various factors that control the magnitude of TMR in MTJs have been reviewed by Evgeny Tsymbal of University of Nebraska-Lincoln and co-workers.

Atom lithography

One-, two-and three-dimensional nanostructures with atom lithography
Markus K Oberthaler and Tilman Pfau
J. Phys.: Condens. Matter
15 No 6 (19 February 2003) R233-R255

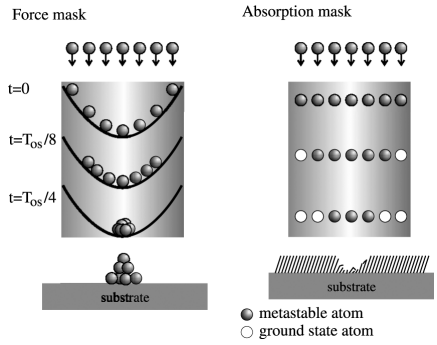

Two types of light masks employed in atom lithography experiments. A well collimated atomic beam impinges onto a light field. A light force mask can be described by a harmonic potential which acts like a lens for matter waves, leading to a locally enhanced growth rate on the substrate. In the case of an absorptive mask no force is present but atoms in the metastable state are pumped to the ground state except at a position where the intensity is very small. Combining this with a resist which is only sensitive to metastable atoms, due to their high internal energy, allows us to transfer this pattern onto a substrate.

The semiconductor industry is still based on optical lithography using light with a wavelength of 157 nm, which limits feature widths to about 100 nm. Alternative lithography techniques, like electron-beam, ion-beam and x-ray lithography can produce nanostructures with a resolution of a few nm. New techniques of nanostructures production are being developed including scanning probe techniques, imprint techniques, self-assembly of structures and atom lithography.

Markus Oberthaler of Konstanz and Tilman Pfau of Stuttgart review the current status in the field of atom lithography. In atom lithography, conversely to light lithography, light acts as a mask and atoms form the pattern. The nanostructures on the surface of a substrate are either formed by the deposited atoms themselves or, in close analogy to photolithography, by using a special resist, sensitive to the atomic beam, and successive etching steps. Since atoms, whose de Broglie wavelength is only a few pm, are imaged onto the surface, diffraction effects are currently not a limiting factor. It discusses in detail how atom–light interaction allows masks for atoms to be formed and the possible nanostructures and limitations of this method.

One-, two- and three-dimensional structures have been produced. The straightforward extension to three-dimensional structuring is a particular strength of this method. Another strength is the possibility of producing long-range (up to mm^2) ordered periodic nanostructures with a feature size of 30 nm and period of 213 nm in the case of chromium.

In future this method will be extended to technologically interesting atomic species such as group III atoms, and combined with epitaxial growth. The successful combination of the field of epitaxial growth and atom optics will open up the way for producing new nanostructured materials with new properties.

Relaxor ferroelectrics

The relaxational properties of compositionally disordered ABO_3 perovskites

George A Samara

J. Phys.: Condens. Matter

15 No 9 (12 March 2003) R367-R411

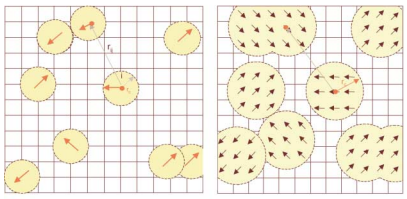

Contrasting the domain structure of a dipolar entity in a normal dielectric host lattice (a) and in a soft FE mode lattice (b). In (a) the dipole polarizes only the region in its immediate vicinity (correlation length $r_c \approx 1$ lattice constant) and behaves as an isolated dipole, whereas in (b) the dipole induces polarization in several unit cells around it (large r_c) forming a dipolar nanodomain.

The ABO_3 perovskite oxides have helped our understanding of ferroelectric and antiferroelectric phenomena. They are prototypical soft phonon mode systems that undergo structural phase transitions involving both polar and non-polar distortions of the cubic lattice.

Random lattice disorder produced by chemical substitution can lead to the formation of dipolar impurities and defects that have a profound influence on their static and dynamic properties. In these highly polarizable host lattices, dipolar entities form polar nanodomains whose size is determined by the dipolar correlation length, r_c, of the host and that exhibit dielectric relaxation in an applied ac field. In the very dilute limit (<0.1 at.%) each domain behaves as a non-interacting dipolar entity with a single relaxation time. At higher concentrations of disorder the domains can interact leading to more complex relaxational behaviour, including the formation of a glass-like relaxor state, or even an ordered ferroelectric state for a sufficiently high concentration of overlapping domains.

George Samara of Sandia National Laboratories reviews these materials, beginning with the simplest cases, namely the relaxational properties of substitutional impurities (e.g., Mn, Fe and Ca) in the quantum paraelectrics $KTaO_3$ and $SrTiO_3$, followed by discussions of the relaxational properties of Li- and Nb-doped $KTaO_3$ and of the strong relaxors in the $PbMg_{1/3}Nb_{2/3}O_3$ and La-substituted $PbZr_{1-x}Ti_xO_3$ families. He discusses the roles of pressure and applied dc biasing electric fields in understanding the physics of these materials including the relaxor-to-ferroelectric crossover.

Relaxors have been one of the 'hot' topics in ferroelectricity during the recent past. The exceptionally large dielectric susceptibilities, electromechanical coupling coefficients and electro-optic constants of perovskite relaxors have been subjects of intense scientific and technological interest. The scientific challenges and technological potential of these materials will ensure that this field will continue to be quite active for the foreseeable future.

Nanomagnetics

R Skomski

J. Phys.: Condens. Matter

15 No 20 (28 May 2003) R841–R896

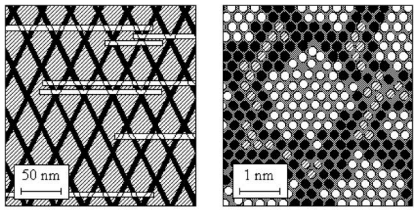

Two schematic bulk nanostructures: (a) sintered Sm–Co and (b) magnetic clusters (white) embedded in a matrix. The two structures are very different from the point of view of size, geometry, origin and functionality. The Sm–Co magnets, consisting of a rhombohedral Sm_2Co_{17}-type main phase (grey), a Cu-rich $SmCo_5$-type grain-boundary phase (black) and a Zr-rich hexagonal Sm_2Co_{17}-type platelet phase (white), are produced by a complicated annealing process and widely used in permanent magnets. Nanostructures such as that shown in (b) can be produced, for example, by mechanical alloying and are used as permanent magnets, soft magnets and magnetoresistive materials.

R Skomski of University of Nebraska, Lincoln reviews magnetic nanostructures, such as dots and dot arrays, nanowires, multilayers and nanojunctions and compares them with bulk magnets. The emphasis is on the physics, but some applications are also outlined, including permanent magnets, soft magnets, magnetic recording media, sensors, and structures and materials for spin electronics. The considered structural length scales range from a few interatomic distances to about one micrometre, bridging the gap between atomic-scale magnetism and the macroscopic magnetism of extended bulk and thin-film magnets. This leads to a rich variety of physical phenomena, including exchange-spring magnetism, random-anisotropy scaling, narrow-wall and constricted-wall phenomena, Curie temperature changes due to nanostructuring and nanoscale magnetization dynamics.

The search for materials with improved intrinsic properties continues to be of scientific and technological interest, but a main thrust of research is the exploitation of artificial nanostructures, yielding materials and functional components not found in nature. An end to the search for new geometries and microchemistries is not yet in sight, and fully realizing the range of magnetic nanostructures and their potential for exploring new applications remains a challenge for future research. The technological progress is accompanied and stimulated by an ever-improving understanding of the magnetic properties of nanostructures. For example, we now understand the crucial effect of imperfections, which largely determine the hysteresis loop and the real-space realization of magnetization processes. In addition to model calculations, full-scale simulations of real structures are now on the horizon, and sophisticated experimental investigation and processing techniques will ensure far-reaching qualitative and quantitative developments.